Materials and Design 32 (2011) 2115–2124

Contents lists available at ScienceDirect

Materials and Design

journal homepage: www.elsevier.com/locate/matdes

Fracture toughness of epoxy/multi-walled carbon nanotube nano-composites under bending and shear loading conditions

M.R. Ayatollahi [a,*], S. Shadlou [a], M.M. Shokrieh [b]

[a] Fatigue and Fracture Research Laboratory, Center of Excellence in Experimental Solid Mechanics and Dynamics, Department of Mechanical Engineering, Iran University of Science and Technology, Narmak, Tehran 16846-13114, Iran
[b] Composites Research Laboratory, Center of Excellence in Experimental Solid Mechanics and Dynamics, Department of Mechanical Engineering, Iran University of Science and Technology, Narmak, Tehran 16846-13114, Iran

ARTICLE INFO

Article history:
Received 12 July 2010
Accepted 16 November 2010
Available online 20 November 2010

Keywords:
I. Brittle fracture
A. Nanomaterials
A. Composites
Polymer matrix

ABSTRACT

The effects of multi-walled carbon nanotubes (MWCNTs) on the mechanical properties of epoxy/MWCNT nano-composites were studied with emphasis on fracture toughness under bending and shear loading conditions. Several finite element (FE) analyses were performed to determine appropriate shear loading boundary conditions for a single-edge notch bend specimen (SENB) and an equation was derived for calculating the shear loading fracture toughness from the fracture load. It was seen that the increase in fracture toughness of nano-composite depends on the type of loading. That is to say, the presence of MWCNTs had a greater effect on fracture toughness of nano-composites under shear loading compared with normal loading. To study the fracture mechanisms, several scanning electron microscopy (SEM) pictures were taken from the fracture surfaces. A correlation was found between the characteristics of fracture surface and the mechanical behaviors observed in the fracture tests.

1. Introduction

Unique atomic structure, very high aspect ratio and extraordinary mechanical properties make carbon nanotubes (CNTs) ideal reinforcing materials in nano-composites. While a significant number of the existing studies have been focused on the stiffness and strength of CNT-reinforced composites [1–6], relatively few research studies have dealt with the fracture behavior of these nano-composites in the presence of a pre-existing crack. A cracked component can be subjected to two modes of in-plane deformation: (1) mode I in which crack faces open without any sliding (see Fig. 1a), and (2) mode II in which crack faces slide normal to the crack front without any opening (see Fig. 1b). Mode I deformation often takes place when a symmetric cracked specimen is subjected to a pure bending or pure tensile loading conditions. Whereas mode II occurs when there are only shear stresses along the crack line. The resistance of a cracked component against brittle fracture under mode I and mode II loading conditions is called mode I and mode II fracture toughness, respectively.

Contradictory reports have been given on how different types of CNTs and different methods of material processing affect mode I fracture toughness (K_{Ic}) of nano-composites. For instance, Gojney et al. [7] produced epoxy/double walled CNT nano-composite by the calendaring technique and measured K_{Ic} of the resulting nano-composite using the compact tension (CT) specimen. Fracture toughness was found to increase 18.5% and 27.7% at a CNT content of 0.1 and 1 wt.%, respectively. In the same way, Thostenson and Chou [8] used the calendaring technique to disperse MWCNTs in epoxy and used single-edge notch bend (SENB) specimen to measure K_{Ic}. According to [8], the maximum K_{Ic} was obtained for 0.2 wt.% of MWCNTs when the gap between the rolls of calendaring machine was 10 μm. However, Zhou et al. [9] reported 17%, 24%, 30% and 4% increase in K_{Ic} by adding 0.1, 0.2, 0.3 and 0.4 wt.% of MWCNTs to the epoxy using sonication. Moreover, few studies dealt with higher weight percents of additives. For instance, fracture toughness was found to decrease 14% with addition of 2 wt.% of MWCNTs [10]. The effects of functionalization of CNTs on mechanical properties including K_{Ic} were also investigated in some studies. For example, Sun et al. [11] added 1 wt.% of pristine and functionalized single wall carbon nanotubes to epoxy resin using sonication technique. Fracture toughness increased 3% and 18% by addition of pristine and functionalized single wall CNT, respectively. Ma et al. [12] used 3-glycidoxypropyltrimethoxysilane as the functionalization agent for MWCNTs. They used sonication to disperse MWCNTs and CT specimen to measure K_{Ic}. They added 0.05, 0.1, 0.25 and 0.5 wt.% of both pristine and functionalized MWCNTs to epoxy. Fracture toughness decreased 2.5%, 15%, 23% and 24% by addition of untreated MWCNTs and increased 2.5%, 6%, 9% and 10% by addition of functionalized MWCNTs, respectively. Furthermore, Park et al. [13] studied the

* Corresponding author. Tel.: +98 21 77240201; fax: +98 21 77240488.
E-mail address: m.ayat@iust.ac.ir (M.R. Ayatollahi).

0261-3069/$ - see front matter © 2010 Elsevier Ltd. All rights reserved.
doi:10.1016/j.matdes.2010.11.034

Nomenclature

a	crack length (mm)	K_{Ic}	mode II stress intensity factor (MPa$\sqrt{m}$)
B	thickness of specimen (mm)	K_{Ic}	mode I fracture toughness (MPa$\sqrt{m}$)
d,L	distances between loads and crack (mm)	K_{IIc}	mode II fracture toughness (MPa$\sqrt{m}$)
d_f	average outer diameter of fiber (nm)	r,θ	crack tip coordinates
E_c	Young's modulus of the composite (GPa)	V_f	volume percent content of the fiber (vol.%)
E_f	Young's modulus of the fiber (GPa)	w	specimen width (mm)
E_m	Young's modulus of the matrix (GPa)	wt.%	weight percent (%)
F	applied force (N)	ε_t	elongation at break (%)
l_f	length of fiber (μm)	σ_c	tensile strength (MPa)
K_I	mode I stress intensity factor (MPa $\sqrt{m}$)	$\sigma_{\theta\theta}$	tangential stress (MPa)

effects of temperature of oxyfluorination of MWCNTs on the surface properties of MWCNTs. The pristine MWCNTs were treated at room temperature and at three other temperatures i.e. 100 °C, 200 °C and 300 °C. The treated MWCNTs were embedded in the epoxy resin and the fracture resistance of the resulting composites was determined by impact and fracture toughness tests. The maximum increase in K_{Ic} (i.e. 24%) was obtained for the nano-composites containing MWCNTs treated at 100 °C. Furthermore, Lachman and Wagner [14] studied the effects of the molecular nature of the interface between an epoxy matrix and MWCNTs on the mechanical properties of the resultant nano-composites by embedding 0.34 wt.% of variously functionalized MWCNTs, namely, pristine, carboxylated, and aminated MWCNTs in epoxy. The pristine and aminated MWCNTs caused the minimum and maximum increase in K_{Ic} i.e. 19% and 83%, respectively. Fracture toughness of nano-composites has been studied in some other papers as well [15–18].

Some researchers have recently investigated the effects of CNTs on mode I and mode II interlaminar fracture toughness of layered nano-composites. For example, Seyhan et al. [19] prepared the matrix resin containing 0.1 wt.% of amino functionalized MWCNTs utilizing the 3-roll milling technique. Then, E-glass non-crimp fabric/MWCNT modified polymer matrix composites were prepared. The MWCNT modified laminates were found to exhibit 8% and 11% higher mode II interlaminar fracture toughness and interlaminar shear strength values, respectively, as compared to the base laminates. However, no significant improvement was observed in the mode I interlaminar fracture toughness values. Meanwhile, Arai et al. [20] have reported 50% and 150% increase in the mode I and mode II fracture toughness of the epoxy/carbon fiber laminates modified by nano-carbon fibers. Moreover, the addition of 5 wt.% of cup-stacked CNT to epoxy increased the interlaminar fracture toughness up to 300% [21]. A review of the papers published on fracture toughness of epoxy/CNT nano-composites shows that almost all of those studies are confined to mode I fracture. Those very few mode II investigations, which are found in the literature, have dealt only with interlaminar fracture of layered nano-composites and not the mode II fracture toughness of basic epoxy/CNT nano-composites. Indeed, mode II and mixed mode fracture of polymers have been studied but only for pure materials like PMMA [22,23] or dental resins [24].

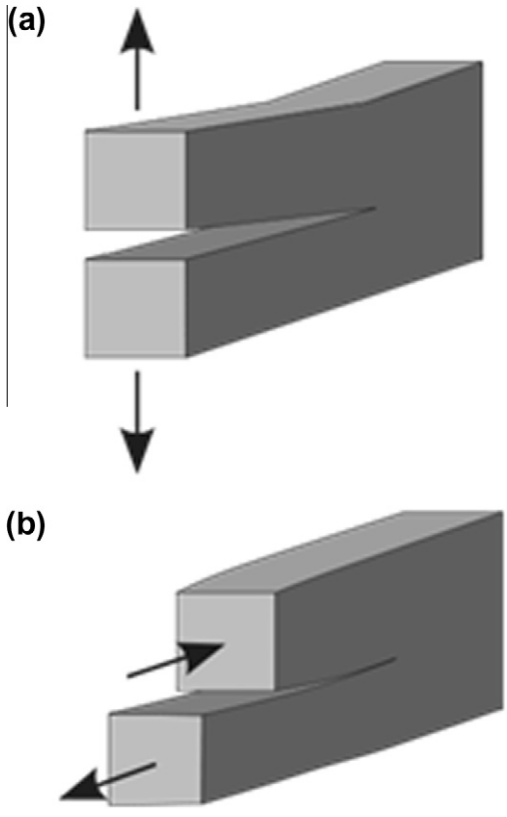

Fig. 1. Schematic of (a) mode I loading conditions (b) mode II loading conditions.

In the present work, fracture toughness under mode I and mode II loading was studied for epoxy/MWCNT nano-composites. First, several finite element (FE) analyses were performed on SENB specimen to determine appropriate boundary conditions for mode II loading. Then, the obtained results were fitted to an equation for calculating mode II stress intensity factor (K_{II}) from the applied load. Afterwards, epoxy/MWCNT nano-composites containing 0.1, 0.5 and 1 wt.% of MWCNTs were prepared using the sonication technique. The tensile and fracture properties were increased by adding MWCNTs except for the elongation at break. The fracture surfaces of the fractured specimens were also examined by scanning electron microscopy (SEM).

2. Finite element analysis

In the present study, the four-point bend specimen (see Fig. 2a) was used for determining pure mode II (i.e. shear loading) fracture resistance of the epoxy/MWCNT nano-composite. When the specimen is subjected to anti-symmetric loading, the amount of bending moment along the crack plane vanishes and there is only a shear force at the crack position. Consequently, the anti-symmetric four-point bend (ASFPB) specimen is often considered as a suitable specimen for mode II fracture tests provided appropriate values are used for the dimensions a, d and L shown in Fig. 2a. The crack parameters for the ASFPB specimen have already been studied by some researchers [25,26]. However, Aliha et al. [27] showed that when the loads F are close to the crack plane the negative T-stresses which are produced in the specimen can affect the experimental results. Moreover, if the distance between the loads F and P i.e. $(L-d)$ is not long enough, the specimen may fracture at a point

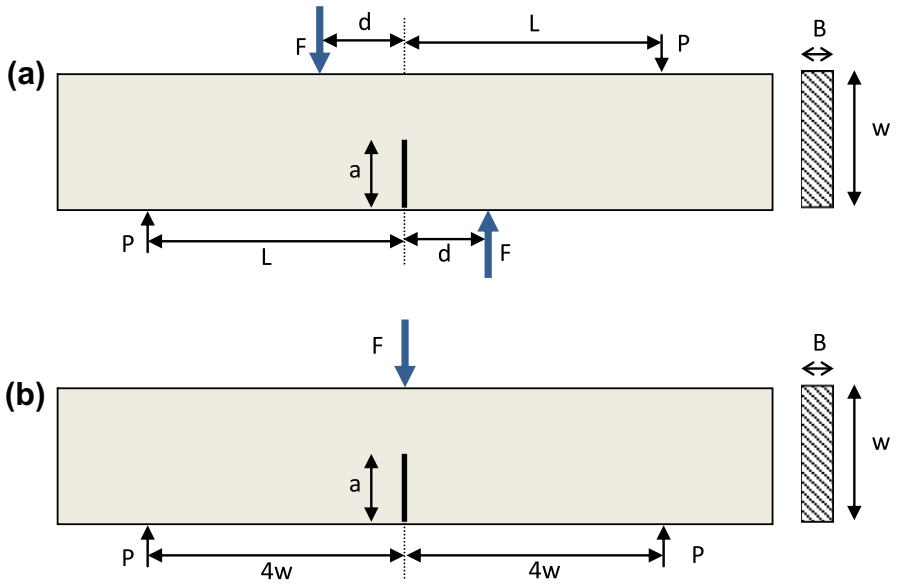

Fig. 2. Mode I and mode II test specimens (a) four-point bend specimen under anti-symmetric loading (pure mode II) (b) three-point bend specimen (pure mode I).

within this distance and not from the crack tip. This is because by moving F towards P, the shearing force along the crack line decreases significantly. Therefore, a series of finite element analyses were performed in order to determine appropriate values for the dimensions a, d and L. To verify the finite element simulation, first a specimen similar to the one analyzed by Fett [25] with $L/w = 2.5$, $B = d = w/2$, $a/w = 0.5$ and $F = 1000$ N was modeled. The mode II stress intensity factor was obtained 0.93 MPa$\sqrt{\text{m}}$ which is very close to 0.97 MPa$\sqrt{\text{m}}$ reported by Fett [25].

Then, for simplicity, L/w and B/w were chosen arbitrarily 2 and 0.5. Our initial fracture experiments showed that for $L/w = 2$ and $B/w = 0.5$, fracture does not initiate from the crack tip if $d/w \geqslant 1$ as elaborated earlier. Therefore, $d/w = 0.75$ was chosen. Then, the crack length was changed and the effect of a/w on K_{II}/K_I ratio was investigated. The results obtained from FE analyses are presented in Fig. 3. It is seen that by increasing a/w, the stress intensity factor ratio K_{II}/K_I increases which is desirable. Meanwhile, when a/w approaches one or zero, the crack tip gets too close to the edges of specimen, resulting in a strong interaction between the local stresses generated by the loads F and the crack tip stresses. Therefore, the best condition in which the crack tip has the maximum distance from the top and bottom edges, occurs when $a/w = 0.5$.

According to Fig. 3, when $a/w = 0.5$ the ratio K_{II}/K_I is equal to 25 which is a good amount for the assumption of pure mode II loading. The mode II stress intensity factor (K_{II}) for the ASFPB specimen can be written as:

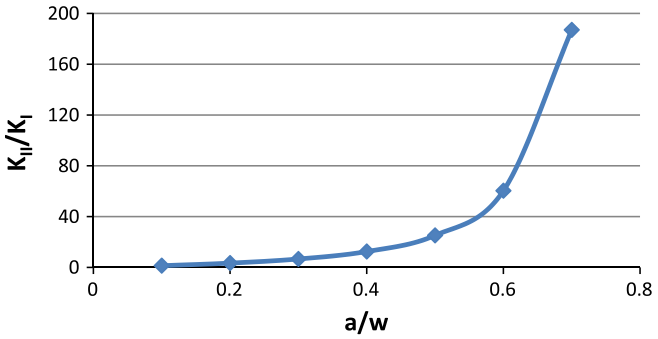

Fig. 3. The variation of K_{II}/K_I ratio versus the crack length ratio a/w.

$$K_{II} = \frac{F}{B \cdot w^{0.5}}\left(1 - \frac{d}{l}\right) f\left(\frac{a}{w}\right) \tag{1}$$

where $f(a/w)$ is a non-dimensional geometry factor. Using Eq. (1) and also the K_{II} values determined by FE analysis for different values of a/w, the following relation was obtained for $f(a/w)$ by fitting a forth order polynomial to the numerical results

$$f\left(\frac{a}{w}\right) = 9.763\left(\frac{a}{w}\right)^4 - 15.036\left(\frac{a}{w}\right)^3 + 8.667\left(\frac{a}{w}\right)^2 + 1.695\left(\frac{a}{w}\right) - 0.037 \quad 0.1 < \left(\frac{a}{w}\right) < 0.7 \tag{2}$$

Since $a/w = 0.5$ was taken for all the specimens used in the fracture experiments, the numerical amount of $f(a/w)$ for $a/w = 0.5$ is 1.71.

The mode I (i.e. pure bending) fracture toughness was determined based on ASTM standard [28] using the three-point bend specimen. For this test, the specimen is subjected to symmetric loading, as shown in Fig. 2b. According to the ASTM standard [28], the mode I fracture toughness can be computed from

$$K_I = \left(\frac{P_{cr}}{BW^{0.5}}\right) f\left(\frac{a}{w}\right) \tag{3}$$

where P_{cr} is the fracture load and $f(a/w)$ can be calculated from

$$f\left(\frac{a}{w}\right) = 6 \times \left(\frac{a}{w}\right)^{0.5} \frac{\left[1.99 - \frac{a}{w}\left(1 - \frac{a}{w}\right)\left(2.15 - 3.93 \times \frac{a}{w} + 2.7 \times \left(\frac{a}{w}\right)^2\right)\right]}{\left(1 + 2 \times \frac{a}{w}\right)\left(1 - \frac{a}{w}\right)^{1.5}} \tag{4}$$

3. Experiment

3.1. Materials and specimen preparation

The epoxy resin ML-506 (Bisphenol F) was selected because of its low viscosity and extensive industrial applications. The low viscosity of the matrix makes the dispersion of additives easier. The curing agent was HA-11 (Polyamine). The SEM pictures showed that the MWCNT diameters were between 30 and 40 nm. According to the supplier, Nanostructured and Amorphous Materials Inc., the MWCNT lengths were between 10 and 30 μm, and the carbon purity was 95%.

Three different types of polymer nano-composites reinforced with 0.1, 0.5 and 1 wt.% MWCNTs were prepared as described

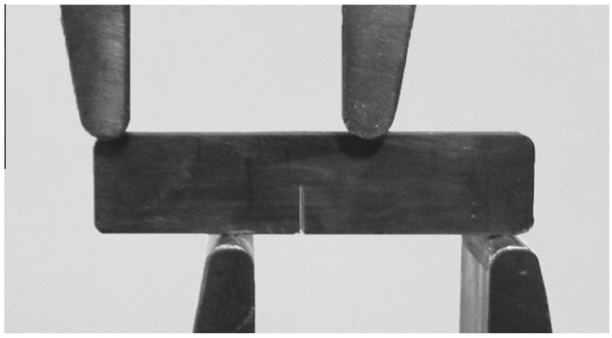

Fig. 4. The cracked specimen in anti-symmetric four-point bend fixture.

below. First, epoxy was mixed with the desired MWCNTs contents and stirred for 25 min at 2000 rpm. Then, the mixtures containing 0.1, 0.5 and 1 wt.% MWCNTs were sonicated for 45 min, 67 min and 90 min, respectively, in order to break the residual aggregates. During the sonication, the mixture container was held in water to keep the temperature of the mixture around 45 °C. In addition, during the sonication the mixture was stirred every 10 min using a small spoon to make sure the sonication energy was applied uniformly to the entire mixture. Afterwards, the hardener was added gradually (i.e. drop by drop) while the mixture was being stirred at 100 rpm to prevent the creation of bubbles as much as possible. Next, the solution was degassed for 20 min in vacuum and casted into differently shaped molds (dog-bone and SENB specimens). Finally, the specimens were cured for 24 h at 25 °C followed by 2 h at 80 °C.

3.2. Mechanical characterization

The Young's modulus, the tensile strength, and the failure strain of the nano-composites were obtained from tensile tests conducted on the dog-bone shaped specimen according to specimen type I in ASTM standard [29]. A Santam universal apparatus with a 50 kN load-cell was used to run the tensile tests. The strain was determined from the data extracted using an extensometer of 50 mm gage length.

Fracture toughness of nano-composite was measured for both pure mode I and pure mode II loading using a $10 \times 20 \times 88$ mm specimen (Fig. 4). First, a primary crack was created in the specimen using a thin saw. Then, the crack tip was sharpened utilizing a razor blade. Since this method of sharpening makes it difficult to determine the exact crack length before the fracture test, the crack length was measured after the fracture test using an optical microscope and a ruler with 100 μm accuracy. The fracture tests were performed using a Santam universal apparatus and a 10 kN load-cell. The fracture load was recorded by the test machine then K_{Ic} and K_{IIc} were computed using Eqs. (3) and (1). For each type of material and each mode of loading, three specimens were tested.

3.3. Electron microscopy

After the mechanical tests, the fracture surfaces of the neat epoxy and the nano-composites were comparatively examined using scanning electron microscopy (SEM) (Tescan VEGA-II SBU) and some information related to the MWCNTs dispersion status and the fracture mechanisms was extracted.

4. Results and discussion

4.1. Tensile properties

The mechanical properties of polymers are generally supposed to be improved by addition of CNTs. The results of the tensile tests are presented in Table 1. Typical stress–strain curves of the pure epoxy and the nano-composites are shown in Fig. 5. Higher filler loading resulted in higher Young's modulus of nano-composite. Increase in Young's modulus with increasing the amount of MWCNT has been reported by other researchers as well [1,3,30]. To compare the results obtained for the Young's modulus with theoretical estimations, the Halpin–Tsai theory for the unidirectional orientation of reinforcements [31] was employed. According to this theory, the maximum obtainable Young's modulus for a composite with a perfect distribution and impregnation with polymer is given by

$$E_c = \left(\frac{3}{8}\frac{1+2\left(\frac{l_f}{d_f}\right)\eta_l V_f}{1-\eta_l V_f}+\frac{5}{8}\frac{1+2\eta_T V_f}{1-\eta_T V_f}\right)E_m \tag{5}$$

Table 1
Tensile properties of pure epoxy and nano-composites.

Elongation at break ε_t (%)	Tensile strength σ_c (MPa)	Young modulus E_C (GPa) (Eq. (5))	Young modulus E_C (GPa) (Exp.)	Samples
3.10 ± 0.17	68.35 ± 2.43	–	3.15 ± 0.14	Pure epoxy
2.98 ± 0.3	71.74 ± 3.32	3.31	3.24 ± 0.25	0.1 wt.% MWCNT
2.87 ± 0.27	73.94 ± 6.17	3.96	3.51 ± 0.18	0.5 wt.% MWCNT
2.70 ± 0.31	72.46 ± 5.24	4.78	3.69 ± 0.30	1 wt.% MWCNT

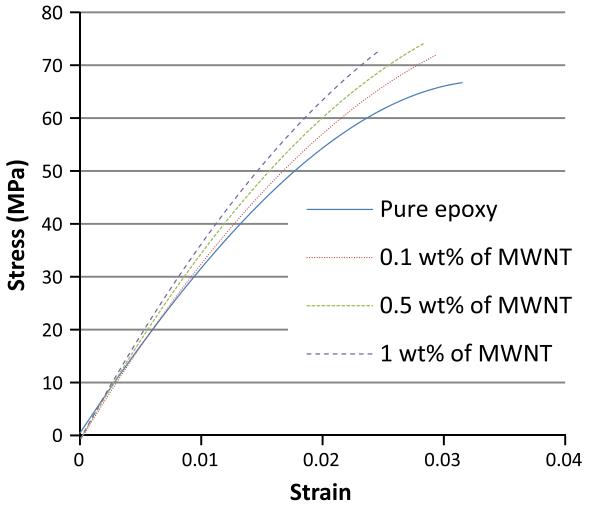

Fig. 5. Typical stress–strain curves for different MWCNT weight percent.

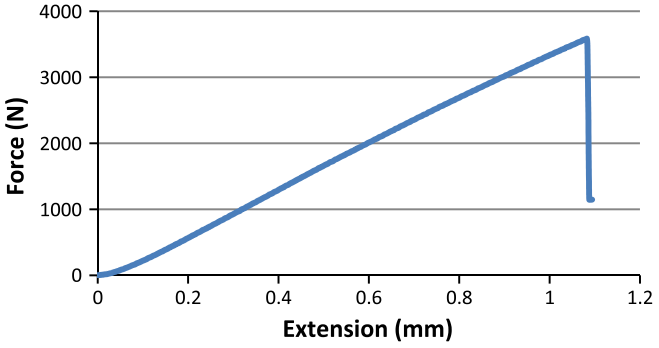

Fig. 6. A typical force–displacement diagram of specimen containing 0.5 wt.% MWCNT under mode II loading conditions.

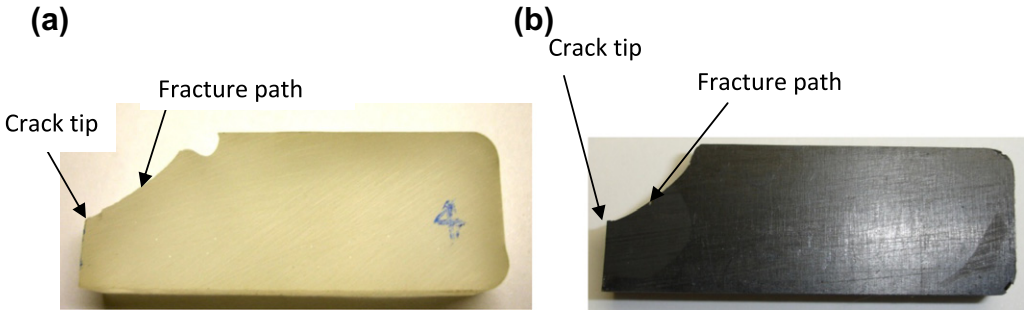

Fig. 7. Samples of specimens broken under mode II loading conditions for (a) pure epoxy (b) epoxy/0.1 wt.% MWCNT.

in which

$$\eta_l = \frac{\frac{E_f}{E_m} - 1}{\frac{E_f}{E_m} + 2\left(\frac{l_f}{d_f}\right)}, \quad \eta_T = \frac{\frac{E_f}{E_m} - 1}{\frac{E_f}{E_m} + 2} \tag{6}$$

where E_C is the Young's modulus of the composite, l_f is the length of MWCNTs, d is the average outer diameter of nanotube, E_{NT} is the Young's modulus of the nanotubes, E_m is the Young's modulus of the epoxy matrix and V_f is the volume content of MWCNTs. According to the properties given by Nanostructured and Amorphous Materials Inc., the average length for the used MWCNT was about 25 μm, E_{NT} was 1 TPa and V_f was equal to 0.052, 0.26 and 0.52 vol.% for 0.1, 0.5 and 1 wt.%, respectively (calculated based on the epoxy density of 1.11 g/cm^3 and the MWCNTs density of 2.1 g/cm^3). The Young's modulus for epoxy was 3.15 GPa. The Young's modulus of nano-composites calculated using Eqs. (5) and (6) are presented in Table 1.

The calculated Young's modulus is in good agreement with the test results only for 0.1 wt.% MWCNTs content which suggests a good dispersion and interfacial strength [32,33]. With increasing the MWCNTs content, the difference between the theoretically predicted and experimentally obtained Young's moduli grows. This is because the theory assumes a uniform dispersion of the filler in the matrix and a flawless bonding [34], while there are still local MWCNT agglomerations within the nano-composite especially in higher contents of filler. In addition, the presence of voids produced during stirring the MWCNTs/epoxy suspension with the hardener, decreases the mechanical properties. Furthermore, by adding more MWCNTs the viscosity of the mixture increases which makes the degassing of mixture more difficult.

The tensile strength values were also improved by adding MWCNTs to epoxy. However, the improvement in tensile strength occurred only when MWCNT was added up to 0.5 wt.%. The presence of more agglomerates in the specimen with 1 wt.% of MWCNTs, as elaborated in the next section, can possibly be the reason for this trend. The correlation between the dispersion status and the mechanical properties is discussed in [35]. Table 1 also shows a reduction in the elongation at break of nano-composites relative to that of pure epoxy, indicating a ductile to brittle trend in nano-composite with increasing the filler loading. A similar finding has been reported in [36] as well. It is noteworthy that different flaws like voids and impurities can reduce the elongation at break as well.

4.2. Fracture toughness

Generally, CNTs are known to improve fracture toughness of epoxies. As mentioned earlier, previous studies have shown that the incorporation of CNTs into epoxy leads to improvements in mode I fracture toughness K_{Ic} of nano-composites [14,37].

In the present study, the three-point bend specimen and the ASFPB specimen were used to determine mode I and mode II fracture toughness, respectively. The force–displacement diagrams for all the specimens in mode I and mode II were linear up to the fracture load, which shows the linear elastic and brittle behavior of the tested materials. A typical force–displacement diagram is shown in Fig. 6 for 0.5 wt.% epoxy/MWCNT nano-composite. While, the mode I specimens fractured all along the direction of initial crack, the crack extension in mode II specimens took place at angles slightly less than 70° from the initial crack. Fig. 7 shows samples of pure epoxy and nano-composite specimens broken under mode II loading conditions.

As described earlier, K_{Ic} and K_{IIc} were determined experimentally using Eqs. (3) and (1), respectively. The obtained results are presented in Table 2. According to Table 2, with addition of MWCNT to epoxy, both K_{Ic} and K_{IIc} increase. Fig. 8 shows the values of increases in K_{Ic} and K_{IIc} of the nano-composite compared to the pure epoxy for different amounts of filler. Two important points can be inferred from Fig. 8. First, regardless of the amount of filler, the presence of MWCNT causes more increase in fracture toughness of epoxy under shear loading compared with mode I loading. The second point is that in mode I loading, fracture toughness of

Table 2
Mode I and mode II fracture toughness of pure epoxy and epoxy/MWCNT nano-composites.

Mode of fracture	Pure epoxy	0.1 wt.% MWCNT	0.5 wt.% MWCNT	1 wt.% MWCNT
Mode I MPa$\sqrt{m}$	1.619 ± 0.14	1.865 ± 0.07	2.045 ± 0.1	1.93 ± 0.19
Mode II MPa$\sqrt{m}$	1.49 ± 0.15	1.815 ± 0.18	2.055 ± 0.2	2.18 ± 0.25

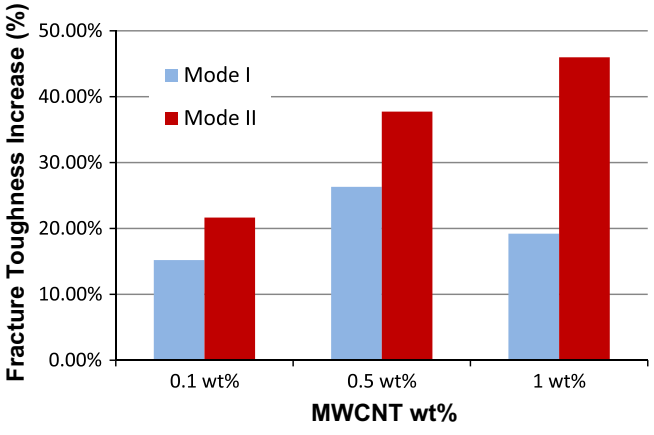

Fig. 8. The increase in mode I and mode II fracture toughness in different amount of contents.

the nano-composite containing 1 wt.% MWCNT is lower than that containing 0.5 wt.% MWCNT while in shear loading the contrary occurs.

4.3. Fractography

To recognize the reasons for the above trend, the fracture mechanisms in mode I and mode II loading were investigated. The fracture surfaces of all specimens were studied using SEM and optical microscopy. Fig. 9 shows typical pictures taken from the mode I specimen surfaces. The smooth fracture surface of the neat epoxy indicates a typical brittle fracture behavior [15,38]. With addition of reinforcement, the fracture surfaces show regular shear steps. Furthermore, the surface roughness increases with higher MWCNT contents suggesting that the crack propagation in the nano-composite was opposed by rigid and stiff MWCNTs. In other words, since the segments of primary crack front had to bend between the tubes, more energy was needed for such a local deviations which leads to an increase in fracture toughness. However, the addition of 1 wt.% of MWCNTs to epoxy decreased K_{Ic} compared to the nano-composite containing 0.5 wt.% of MWCNTs. Besides, in the 1 wt.% MWCNT nano-composite the regularity of shear steps is lost (see Fig. 9d) which can be due to MWCNT agglomerates. For a more detailed investigation, high magnification pictures were also taken from the fracture surfaces (Fig. 10). This pictures revealed that in lower contents of MWCNTs (i.e. 0.1 and 0.5 wt.%)

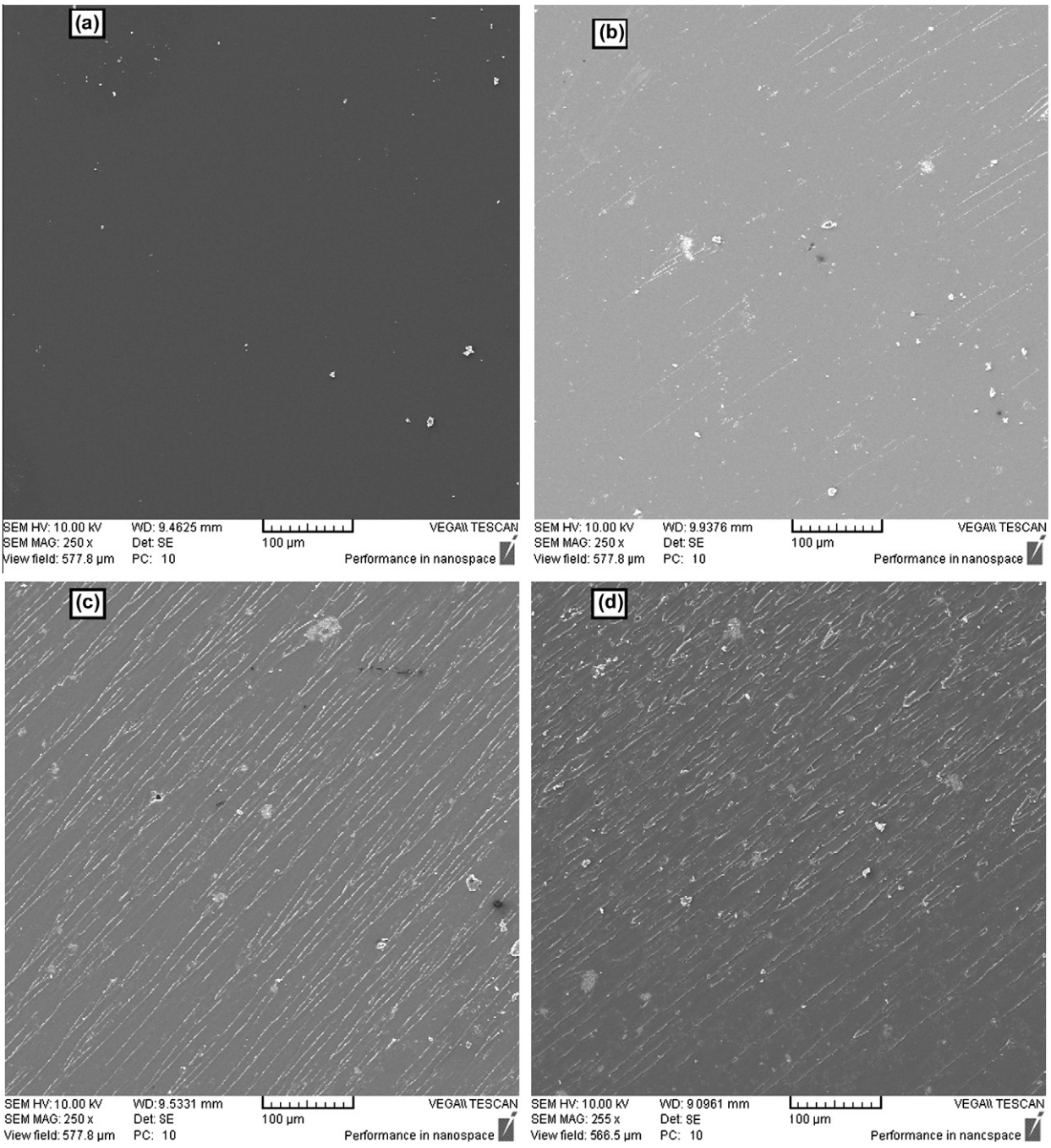

Fig. 9. Mode I fracture surfaces of (a) neat epoxy (b) 0.1 wt.% MWCNT/epoxy (c) 0.5 wt.% MWCNT/epoxy (d) 1 wt.% MWCNT/epoxy near the region of fracture initiation. The direction of crack propagation is from top right to bottom left.

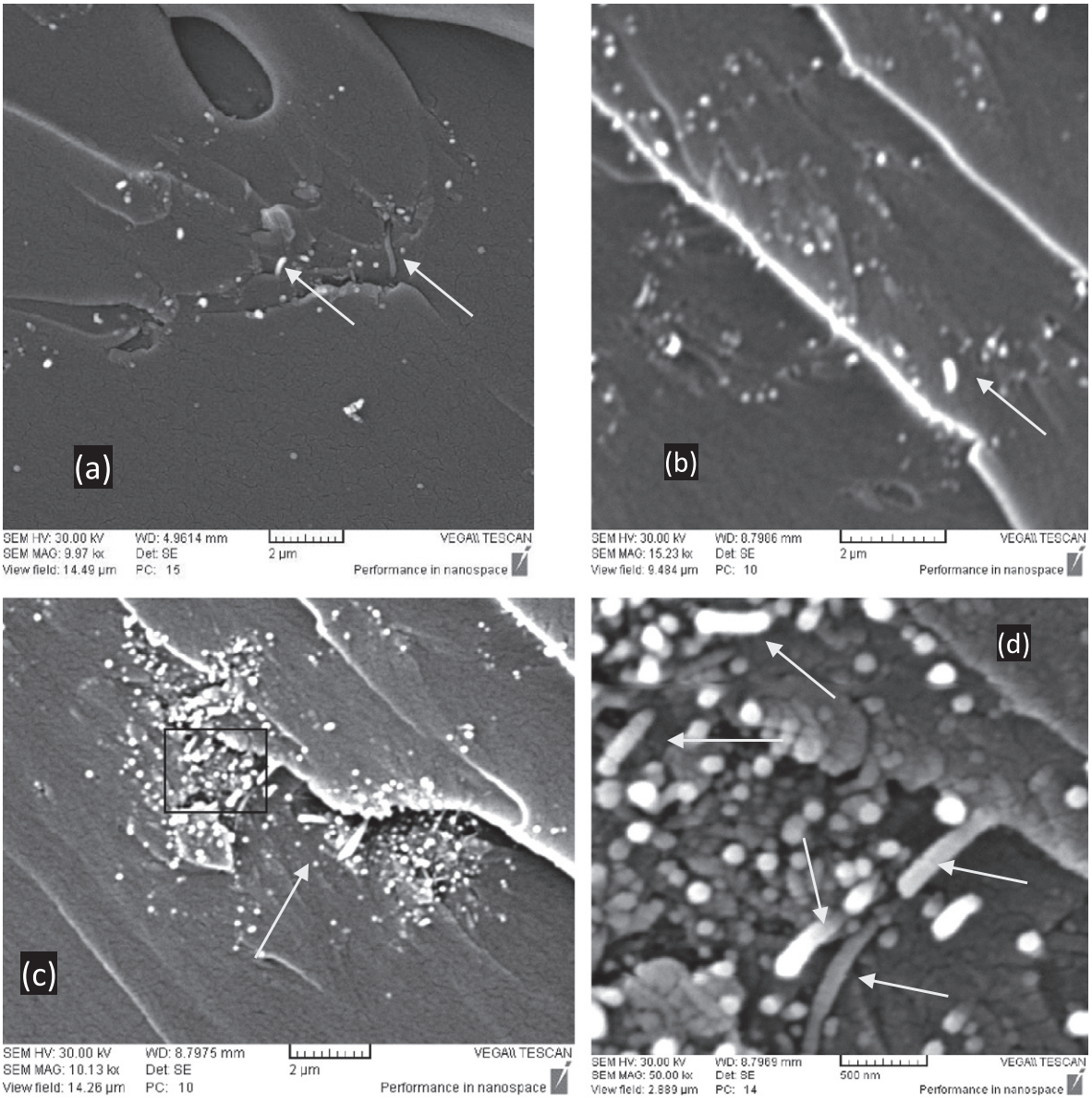

Fig. 10. SEM micrographs of fracture surfaces for epoxy/MWCNT nano-composites (a) 0.1 wt.% (b) 0.5 wt.% (c) 1 wt.% (d) magnification of a selected part in (c) near the region of crack propagation. The direction of fracture initiation is from top right to bottom left.

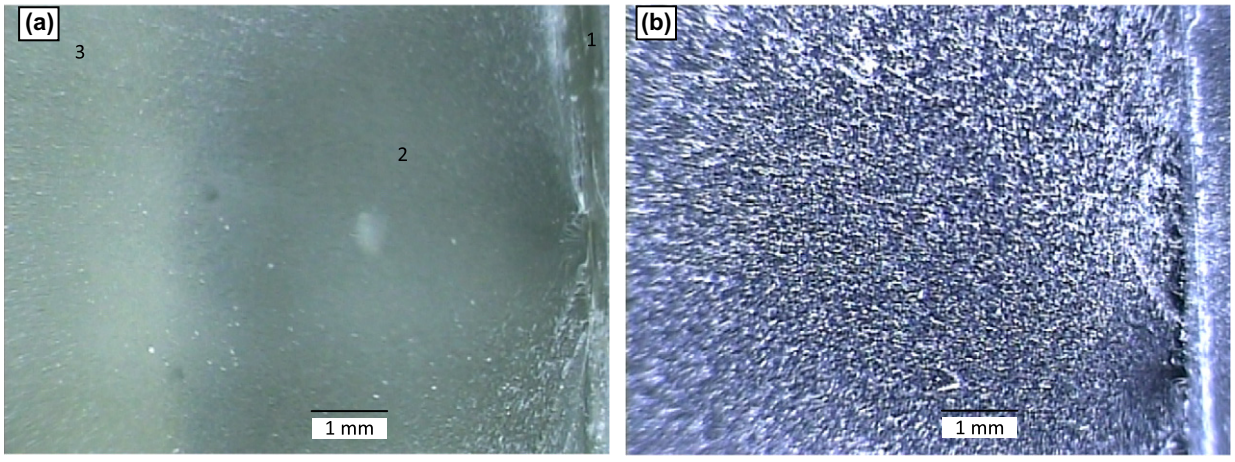

Fig. 11. Optical microscopy pictures of mode II fracture surfaces (a) neat epoxy (b) 0.5 wt.% MWCNT/epoxy. The direction of crack propagation is from right to left.

there is a well dispersion of fillers (Fig. 10a and b). Meanwhile, as shown in Fig. 10c, in specimens containing 1.0 wt.% of enhancers, MWCNTs tended to be agglomerated. However, a more detailed study of the observed agglomerations revealed that the resin had penetrated into and wet the MWCNTs accumulation. It is noteworthy to mention that the signs of aggregation are observable even in low magnification pictures. Fig. 9d shows that in the areas where MWCNTs are aggregated, the regular pattern of steps is affected and the tail-like structures are formed. These agglomerations can be responsible for reduction of tensile strength and K_{Ic} of nanocomposite in 1 wt.% of MWCNTs which was mentioned earlier. It is noteworthy that the measured diameter of MWCNTs taken out of epoxy is almost twice its original value prior to embedment. A similar observation has also been reported by Lachman and Daniel Wagner [14] who suggested that the observed diameter enhancement can be due to epoxy coating, i.e. a cylindrical bulk of epoxy surrounding MWCNT is also pull out of the matrix together with MWCNT itself. In fact, this epoxy coating can also be a sign of good adhesion between MWCNT and the epoxy.

In all specimens, some MWCNTs are seen pulled out of the fracture surface (shown by white arrows) indicating a bridging mechanism. Bridging mechanism plays an important role in improving the fracture toughness of composites [16]. For instance, Shukla and Parameswaran [39] showed that crack bridging of alumina platelets with an aspect ratio between 25 and 50 had a great influence on delaying the crack propagation in epoxy. Generally, the number of pulled out MWCNTs in accumulation parts are more than those in the well-dispersed parts. This behavior can be due

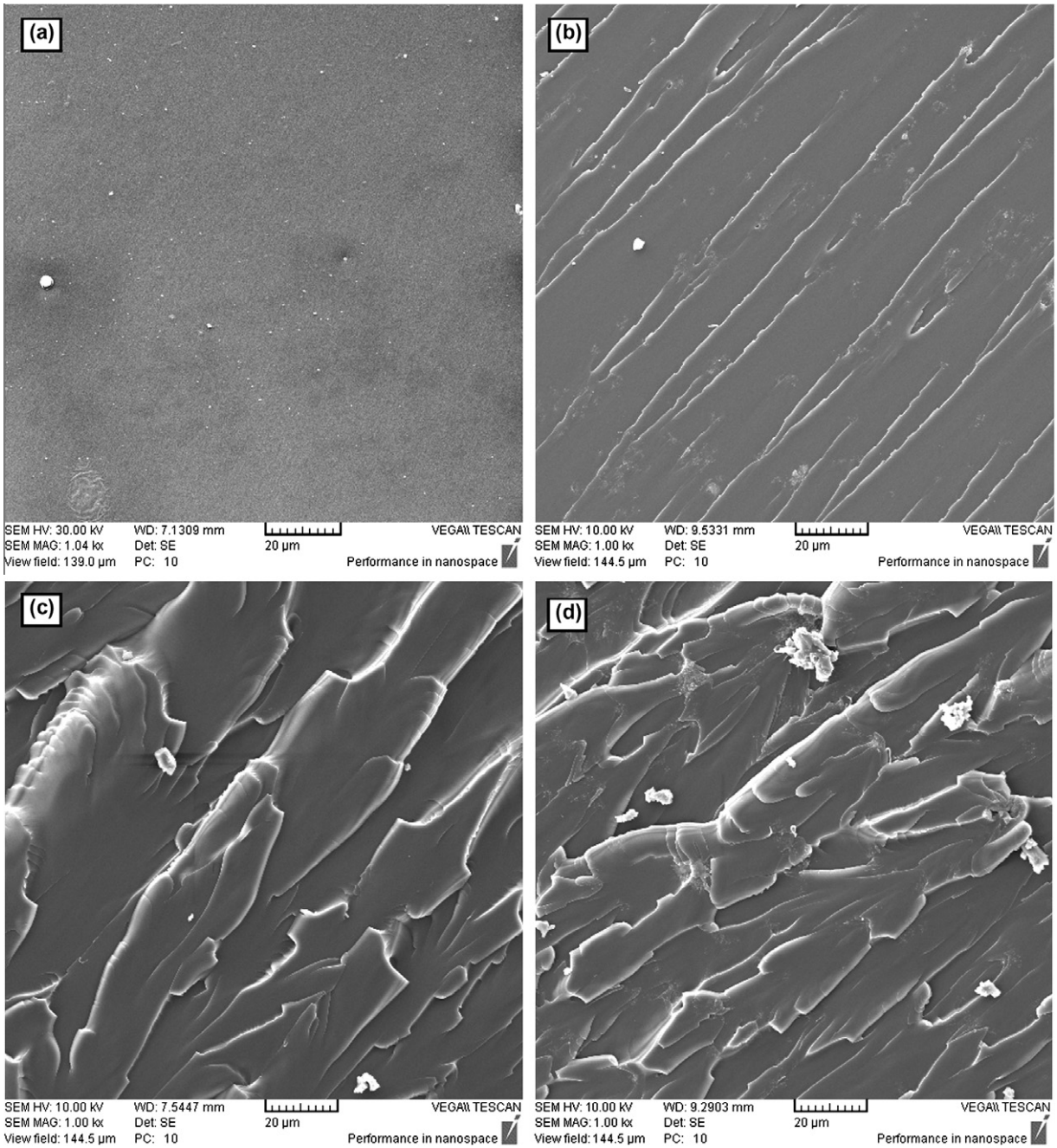

Fig. 12. SEM pictures of mode I fracture surfaces (a) neat epoxy (b) 0.5 wt.% MWCNT/epoxy and mode II fracture surfaces (c) neat epoxy (d) 0.5 wt.% MWCNT/epoxy near the region of crack propagation. The direction of fracture initiation is from top right to bottom left.

to a weaker interface between MWCNTs and polymer in these areas, which makes it easier for MWCNTs to come out of the polymer matrix. The pulled out MWCNTs show that these agglomerates participate in toughening mechanisms and that they can be of different effects on the mechanical properties of nano-composites.

The specimens broken under mode II (shear) loading conditions were also investigated. First, the fracture surfaces of specimens were studied using optical microscopy (Fig. 11). As described earlier, for pure epoxy under mode I loading the fracture surface included a mirror like region. However, in shear loading there is also a rough and misty area particularly near the initial crack front, in addition to the mirror-type area, as shown in Fig. 11a. The responsible phenomena for the formation of these areas are discussed in [40]. For instance, Bhattacharjee and Knott [40] have shown that by shifting from pure mode I to pure mode II, the level of stress ahead of the crack tip becomes larger. The presence of these higher stresses in shear loading can be one reason for misty areas in mode II fracture surfaces, because at some stages of crack growth the stress becomes high enough to initiate secondary local cracks [39,40] that give rise to the rough area next to the initial crack front. Another reason for higher roughness of surfaces under shear loading is the fact that in shear loading unlike normal loading, fracture does not take place along the initial pre-crack. In addition, once fracture initiates at an angle θ_0, it does not grow in a straight plane and the crack path profile is curved (as shown in Fig. 7). The curved path of crack growth can be due to the fact that the maximum tangential stress direction changes as the crack propagates. Thus, at each step of crack propagation, the crack plane rotates and grows in a new direction which has the maximum tangential stress [40]. The crack plane rotation can also be another reason for the misty and rough fracture surfaces in the specimens fractured under mode II loading.

A similar study for the mode II fracture surfaces of nano-composites containing 0.5 wt.% MWCNTs, revealed that, the roughness of the nano-composites surfaces was significantly more than that of pure epoxy. This increase in the surface roughness of nano-composites caused a uniform rough surface across the fracture surface (Fig. 11b).

While some of the mechanisms observed in mode I fracture can participate in mode II fracture as well, there might be some other mechanisms responsible for more increase in fracture toughness of nano-composites under shear loading. For example, the creation of secondary cracks due to higher stresses along the crack front under shear loading, which was explained earlier, can provide an extra opportunity for MWCNTs to dissipate more energy because more local crack nucleation require higher fracture energy participating in the presence of MWCNTs. Moreover, as mentioned earlier, during the propagation of crack under shear loading the crack plane constantly changed. The presence of stiff MWCNTs in each step of crack plane rotation provides a higher resistance against crack propagation. Fig. 12 shows the mode I and mode II fracture surfaces with higher magnification. It is seen that the mode I fracture surfaces (Fig. 12a and b) of both pure and enhanced epoxy are generally much smoother than the mode II fracture surfaces (Fig. 12c and d). While just some shallow scratches are seen in mode I fracture surfaces of epoxy/0.5 wt.% MWCNT nano-composite, there are deep cleavages in both pure and enhanced epoxy surfaces related to mode II fracture. In nano-composites broken under mode II loading, there are also some shallow cleavages and dendriform cracks (Fig. 12d). The deep cleavages observed for both pure and enhanced epoxy in mode II specimens can be due to changing of crack plane. The shallow cleavages, which were observed in both mode I and mode II fracture surfaces of the nano-composites, might be because of both the creation of secondary cracks and the crack deviation mechanisms discussed earlier for mode I fracture.

As stated earlier, the mode I fracture toughness of nano-composites containing 1 wt% MWCNT was lower than those containing 0.5 wt.% MWCNT which was attributed to aggregates observed in the former. However, the opposite happened in shear loading conditions. This opposing behavior might be due to the extra energy dissipating mechanisms under shear loading compared to fracture under mode I loading, which outweigh the negative effects of agglomeration. Moreover, a possible reason for the mentioned trend might be the fact that larger agglomerates are able to interact with crack front more effectively under shear loading.

5. Conclusions

In the present study, especial emphasis was placed on fracture toughness of epoxy/MWCNTs nano-composites under mode I and mode II loading conditions. Numerous FE analyses were performed and an equation presented using which K_{II} could be calculated in terms of applied load. Three different contents of MWCNT namely, 0.1, 0.5 and 1 wt.% were used in this study. While the maximum mode I fracture toughness was obtained in nano-composites containing 0.5 wt.% of MWCNT, the addition of MWCNTs improved the strength and mode II fracture toughness of epoxy continually. In addition, the presence of MWCNTs had a greater effect on the enhanced fracture toughness of nano-composites under shear loading compared with normal loading. To discover the reason, the fracture surfaces of different specimens were studied and some fracture mechanisms in each loading conditions were recognized. It was found that in addition to the mechanisms that are participating in increasing of the fracture energy under mode I lading, there are some other mechanisms in fracture under shear loading. Moreover, some correlations between the fracture mechanisms and fracture surfaces were observed.

References

[1] Tai NH, Yeh MK, Liu JH. Enhancement of the mechanical properties of carbon nanotube/phenolic composites using a carbon nanotube network as the reinforcement. Carbon 2004;42:2774–7.
[2] Blond D, Barron V, Ruether M, Ryan KP, Nicolosi V, Blau WJ, et al. Enhancement of modulus, strength, and toughness in poly(methyl methacrylate)-based composites by the incorporation of poly(methyl methacrylate)-functionalized nanotubes. Adv Funct Mater 2006;16:1608–14.
[3] Montazeri A, Javadpour J, Khavandi A, Tcharkhtchi A, Mohajeri A. Mechanical properties of multi-walled carbon nanotube/epoxy composites. Mater Des 2010;31:4202–8.
[4] Bal S. Experimental study of mechanical and electrical properties of carbon nanofiber/epoxy composites. Mater Des 2010;31:2406–13.
[5] Montazeri A, Khavandi A, Javadpour J, Tcharkhtchi A. Viscoelastic properties of multi-walled carbon nanotube/epoxy composites using two different curing cycles. Mater Des 2010;31:3383–8.
[6] Bogdanovich AE, Bradford PD. Carbon nanotube yarn and 3-D braid composites. Part I: Tensile testing and mechanical properties analysis. Composite Part A 2010;41:230–7.
[7] Gojny FH, Wichmann MHG, Köpke U, Fiedler B, Schulte K. Carbon nanotube-reinforced epoxy-composites: Enhanced stiffness and fracture toughness at low nanotube content. Compos Sci Technol 2004;64:2363–71.
[8] Thostenson ET, Chou TW. Processing–structure–multi-functional property relationship in carbon nanotube/epoxy composites. Carbon 2006;44:3022–9.
[9] Zhou Y, Pervin F, Lewis L, Jeelani S. Fabrication and characterization of carbon/epoxy composites mixed with multi-walled carbon nanotubes. Mater Sci Eng, A 2008;475:157–65.
[10] Gryshchuk O, Karger-Kocsis J, Thomann R, Kónya Z, Kiricsi I. Multiwall carbon nanotube modified vinylester and vinylester-based hybrid resins. Composite Part A 2006;37:1252–9.
[11] Sun L, Warren GL, O'Reilly JY, Everett WN, Lee SM, Davis D, et al. Mechanical properties of surface-functionalized SWCNT/epoxy composites. Carbon 2008;46:320–8.
[12] Ma PC, Kim J-K, Tang BZ. Effects of silane functionalization on the properties of carbon nanotube/epoxy nanocomposites. Compos Sci Technol 2007;67:2965–72.
[13] Park SJ, Jeong HJ, Nah C. A study of oxyfluorination of multi-walled carbon nanotubes on mechanical interfacial properties of epoxy matrix nanocomposites. Mater Sci Eng, A 2004;385:13–6.

[14] Lachman N, Daniel Wagner H. Correlation between interfacial molecular structure and mechanics in CNT/epoxy nano-composites. Composite Part A 2010;41:1093–8.
[15] Ganguli S, Bhuyan M, Allie L, Aglan H. Effect of multi-walled carbon nanotube reinforcement on the fracture behavior of a tetrafunctional epoxy. J Mater Sci 2005;40:3593–5.
[16] Gojny FH, Wichmann MHG, Fiedler B, Schulte K. Influence of different carbon nanotubes on the mechanical properties of epoxy matrix composites – A comparative study. Compos Sci Technol 2005;65:2300–13.
[17] Hedia HS, Allie L, Ganguli S, Aglan H. The influence of nanoadhesives on the tensile properties and Mode-I fracture toughness of bonded joints. Eng Fract Mech 2006;73:1826–32.
[18] Yu N, Zhang ZH, He SY. Fracture toughness and fatigue life of MWCNT/epoxy composites. Mater Sci Eng, A 2008;494:380–4.
[19] Tugrul Seyhan A, Tanoglu M, Schulte K. Mode I and mode II fracture toughness of E-glass non-crimp fabric/carbon nanotube (CNT) modified polymer based composites. Eng Fract Mech 2008;75:5151–62.
[20] Arai M, Noro Y, Sugimoto Ki, Endo M. Mode I and mode II interlaminar fracture toughness of CFRP laminates toughened by carbon nanofiber interlayer. Compos Sci Technol 2008;68:516–25.
[21] Yokozeki T, Iwahori Y, Ishibashi M, Yanagisawa T, Imai K, Arai M, et al. Fracture toughness improvement of CFRP laminates by dispersion of cup-stacked carbon nanotubes. Compos Sci Technol 2009;69:2268–73.
[22] Aliha MRM, Ayatollahi MR. Geometry effects on fracture behaviour of polymethyl methacrylate. Mater Sci Eng, A 2010;527:526–30.
[23] Ayatollahi MR, Aliha MRM, Hassani MM. Mixed mode brittle fracture in PMMA – An experimental study using SCB specimens. Mater Sci Eng A 2006;417:348–56.
[24] Aliha MRM, Ayatollahi MR. On mixed-mode I/II crack growth in dental resin materials. Scripta Mater 2008;59:258–61.
[25] Fett T. Stress intensity factors for edge crack subjected to mixed mode four-point bending. Theor Appl Fract Mech 1991;15:99–104.
[26] Araki W, Nemoto K, Adachi T, Yamaji A. Fracture toughness for mixed mode I/II of epoxy resin. Acta Mater 2005;53:869–75.
[27] Aliha MRM, Ayatollahi MR, Kharazi B. Mode II brittle fracture assessment using ASFPB specimen. Int J Fract 2009;159:241–6.
[28] ASTM standard test methods for planestrain fracture toughness and strain energy release rate of plastic materials. D5045-99. 100 Barr Harbor Drive, PO Box C700, West Conshohocken, PA 19428-2959, United States; 1999.
[29] ASTM standard test method for tensile properties of plastics. D 638-99. 100 Barr Harbor Drive, West Conshohocken, PA 19428-2959, United States: ASTM; 1999.
[30] Yeh M, Tai N, Liu J. Mechanical behavior of phenolic-based composites reinforced with multi-walled carbon nanotubes. Carbon 2006;44:1–9.
[31] Mallick PK. Fiber reinforced composite materials manufacturing and design. 3rd ed. Taylor & Francis, Inc.; 2008.
[32] Song YS, Youn JR. Influence of dispersion states of carbon nanotubes on physical properties of epoxy nanocomposites. Carbon 2005;43:1378–85.
[33] Bal S. Dispersion and reinforcing mechanism of carbon nanotubes in epoxy nanocomposites. Bull Mater Sci 2010;33:27–31.
[34] Gojny F. Carbon nanotube-reinforced epoxy-composites: Enhanced stiffness and fracture toughness at low nanotube content. Compos Sci Technol 2004;64:2363–71.
[35] Fraczek A, Blazewicz S. Effect of dispersion of carbon nanotubes in polyacrylonitrile matrix on mechanical and thermal behavior of nanocomposites. J Phys Conf Ser 2009:146.
[36] Satapathy BK, Weidisch R, Pötschke P, Janke A. Tough-to-brittle transition in multiwalled carbon nanotube (MWNT)/polycarbonate nanocomposites. Compos Sci Technol 2007;67:867–79.
[37] Chen YL, Liu B, He XQ, Huang Y, Hwang KC. Failure analysis and the optimal toughness design of carbon nanotube-reinforced composites. Compos Sci Technol 2010;70:1360–7.
[38] Zhang X-H, Zhang Z-H, Xu W-J, Chen F-C, Deng J-R, Deng X. Toughening of cycloaliphatic epoxy resin by multiwalled carbon nanotubes. J Appl Polym Sci 2008;110:1351–7.
[39] Shukla DK, Parameswaran V. Epoxy composites with 200 nm thick alumina platelets as reinforcements. J Mater Sci 2007;42:5964–72.
[40] Bhattacharjee D, Knott JF. Effect of mixed mode I and II loading on the fracture surface of polymethyl methacrylate (PMMA). Int J Fract 1995;72:359–81.